

Quantitative assessment of diffusion kurtosis imaging depicting deep myometrial invasion: a comparative analysis with diffusion-weighted imaging

Jia-Cheng Song 

Shan-Shan Lu 

Jing Zhang 

Xi-Sheng Liu 

Cheng-Yan Luo 

Ting Chen 

PURPOSE

We aimed to investigate histogram analysis of diffusion kurtosis imaging (DKI) and conventional diffusion-weighted imaging (DWI) to distinguish between deep myometrial invasion and superficial myometrial invasion in endometrial carcinoma (EC).

METHODS

A total of 118 pathologically confirmed EC patients with preoperative DWI were included. The data were postprocessed with a DKI (b value of 0, 700, 1400, and 2000 s/mm²) model for quantitation of apparent diffusion values (D) and apparent kurtosis coefficient values (K) for non-Gaussian distribution. The apparent diffusion coefficient (ADC) was postprocessed with a conventional DWI model (b values of 0 and 800 s/mm²). A whole-tumor analysis approach was used. Comparisons of the histogram parameters of D , K , and ADC were carried out for the deep myometrial invasion and superficial myometrial invasion subgroups. Diagnostic performance of the imaging parameters was assessed.

RESULTS

The D_{mean} , $D_{10\text{th}}$, and $D_{90\text{th}}$ in deep myometrial invasion group were significantly lower than those in superficial invasion group ($P < 0.001$, $P < 0.001$, and $P = 0.023$, respectively), as well as the ADC_{mean} , $ADC_{10\text{th}}$, and $ADC_{90\text{th}}$ ($P = 0.001$, $P = 0.001$, and $P = 0.042$, respectively). The K_{mean} and $K_{90\text{th}}$ were significantly higher in deep invasion group than those in superficial myometrial invasion group ($P = 0.002$ and $P = 0.026$, respectively). The $D_{10\text{th}}$, K_{mean} , and $ADC_{10\text{th}}$ had a relatively higher area under the curve (AUC) (0.72, 0.66, and 0.71, respectively) than other parameters for distinguishing deep myometrial invasion of EC. $D_{10\text{th}}$ showed a relatively higher AUC than $ADC_{10\text{th}}$ for the differentiation of lesions with deep myometrial invasion from those with superficial myometrial invasion (0.72 vs. 0.71), but the variation was not statistically significant ($P = 0.35$).

CONCLUSION

Distribution of DKI and conventional DWI parameters characterized by histogram analysis may represent an indicator for deep myometrial invasion in EC. Both DKI and DWI models showed relatively equivalent effectiveness.

Worldwide, endometrial carcinoma (EC) is a commonly diagnosed gynecological malignancy (1). A previous study showed that tumors of high histological grade and extensive myometrial invasion with positive lymph node metastasis are associated with poor prognosis (2). Specifically, the depth of the myometrial invasion is strongly connected to the existence of lymph node metastasis and overall patient survival rate (3). In EC with superficial myometrial invasion, the incidence of lymph node metastasis was 3% (4). However, that rate increased to 46% in EC with deep myometrial invasion (5, 6). Furthermore, European groups have advocated a less aggressive surgical approach in superficial myometrial invasion patients for fewer procedure complications (7). Therefore, an accurate assessment of deep myometrial invasion of EC is of great importance in treatment planning (8).

Diffusion-weighted imaging (DWI) has been extensively utilized in the preoperative staging of EC, which includes the accurate assessment of myometrial and cervical invasion as well as lymph node metastasis (9–11). Previous reports have shown that apparent diffusion coefficient (ADC) values of EC are associated with tumor differentiation and degree of myo-

From the Departments of Radiology (J.C.S., S.S.L., J.Z., X.S.L., T.C. ✉ chent19811@163.com) and Gynecology and Obstetrics (C.Y.L.), First Affiliated Hospital of Nanjing Medical University, Nanjing, China.

Received 16 November 2018; revision requested 01 February 2019; last revision received 23 May 2019; accepted 26 June 2019.

Published online 2 January 2020.

DOI 10.5152/dir.2019.18366

You may cite this article as: Song JC, Lu SS, Zhang J, Liu XS, Luo CY, Chen T. Quantitative assessment of diffusion kurtosis imaging depicting deep myometrial invasion: a comparative analysis with diffusion-weighted imaging. *Diagn Interv Radiol* 2020; 26:74–81.

metrial invasion, as well as lymph node metastasis (12–14). Some, however, reported no relationship between tumor ADC values and the depth of myometrial invasion (15). In our opinion, the possible explanations for this discrepancy may be summarized as either relatively limited number of cases in these studies or a different method of region of interest (ROI) delineation or mean ADC value used. Hence, we increased our number of cases and adopted a volume-based histogram analysis to further investigate the diagnostic effectiveness of ADC values in differentiating deep myometrial invasion. The conventional DWI model describes the displacement of water molecules as free diffusion in a Gaussian distribution fitted with a conventional mono-exponential model. In biological tissues, a variety of compartments (e.g., intracellular and extracellular spaces) and barriers (e.g., cell membranes) restrict water molecular diffusion (16). Diffusion kurtosis imaging (DKI), first described by Jensen in 2005, is a non-Gaussian distribution DWI model that was fitted with a bio-exponential model (17). This novel model has been shown to more accurately assess the microstructural complexity of living tissues compared with the mono-exponential fitted DWI model, using kurtosis imaging as an index in the characterization of lesions in the breast, prostate, head, and neck (18–21). To the best of our knowledge, there is limited literature available regarding the application of DKI to identify the depth of myometrial invasion in EC.

Therefore, the present study aimed to assess the relevance of using tumor volume-based histogram analysis of DKI, as well as conventional DWI in elucidating the

depth of myometrial invasion of EC; and to compare the diagnostic efficacy of the DKI model and the conventional DWI model.

Methods

Patient selection

This investigation was a retrospective study and was approved by our institutional review board. The informed consent requirement was waived. A total of 137 consecutive subjects with EC, verified by pipette biopsy or curettage, had a typical pelvic MRI evaluation prior to an operation from January 2016 to December 2017. There was a median of 9 days between the MRI evaluation and the operation (3–16 days). Inclusion criteria for patients were: a) a recent diagnosis of EC without prior chemotherapy or radiotherapy, b) total hysterectomy and bilateral salpingo-oophorectomy conducted in our hospital, c) available histopathological tumor type (endometrioid or non-endometrioid carcinoma), tumor differentiation, depth of myometrial invasion, lymphovascular invasion and lymph node metastasis after surgery, d) DKI conducted on a 3.0T MRI scanner using b values of 0, 700, 1400, and 2000 s/mm^2 , as well as DWI performed with b values of 0 and 800 s/mm^2 . We excluded 19 patients because of unsatisfactory image quality ($n=12$) or unidentifiable tumor size on DWI or T2-weighted images (tumor volume $<1\text{ cm}^3$) ($n=7$). A total of 118 patients (mean age, 55.70 ± 9.31 years; range, 34–76 years) were enrolled in this study.

MRI protocol

All of the MRI examinations were performed using a 3.0 Tesla scanner (Magnetom Verio, Siemens Healthineer) that was equipped with a 16-channel body phase array coil. The MRI protocols included in this study were as follows: Sagittal T2-weighted turbo spin-echo sequence (repetition time [TR]/echo time [TE], 4520/125 ms; section thickness, 3 mm; intersection gap, 0.3 mm; field of view (FOV), $250 \times 250\text{ mm}^2$; and matrix, 384×336), fat-suppression coronal T2-weighted turbo spin-echo sequence (TR/TE, 4000/77 ms; section thickness, 3 mm; intersection gap, 0.3 mm; FOV, $300 \times 300\text{ mm}^2$; and matrix, 384×336), as well as an axial T2-weighted turbo spin-echo sequence (TR/TE, 4330/129 ms; section thickness, 3 mm; intersection gap, 0.3 mm; FOV, $250 \times 250\text{ mm}^2$; and matrix, 384×336). Finally, a transverse T1-weighted turbo spin-echo

sequence (TR/TE, 993/25 ms; section thickness, 3 mm; intersection gap, 0.3 mm; FOV, $250 \times 250\text{ mm}^2$; and matrix, 384×336) was performed. DWI and DKI were conducted based on a transverse single-shot echo-planar sequence (TR/TE, 6400/78 ms; section thickness, 3 mm; intersection gap, 0.3 mm; FOV, 25 cm; matrix, 192×130 ; Grappa, 2 and 19 sections) in three orthogonal directions with two spectra of b values: (0 and 800 s/mm^2) and (0, 700, 1400, and 2000 s/mm^2). Finally, dynamic contrast-enhanced sagittal T1-weighted imaging was conducted based on a FLASH (fast low angle shot) sequence (TR/TE, 5.32/1.85 ms; section thickness, 3 mm; intersection gap, 0.3 mm; FOV, $250 \times 250\text{ mm}^2$; matrix, 256×256). A dosage of 0.1 mmol/kg of gadolinium-diethylene triamine pentaacetic acid (Magnevist; Bayer Schering Pharma AG) was given at a rate of 3.5 mL/s. This was accompanied by a 20 mL bolus of saline given at the identical rate.

Data processing

All of the DWI data were transmitted from a PACS workstation (Centricity PACS 3.1.1.4, GE Healthcare) in DICOM format to an independent personal computer for further analysis. All of the DWI and DKI post-processing procedures were performed with internally created software (Fire Voxel; CAI[®]R) using the following two basic diffusion-related equations:

$$S(b) = S_0 \cdot \exp(-b \cdot ADC) \quad (1)$$

$$S(b) = S_0 \cdot \exp\left(-b \cdot D + \frac{b^2 D^2 K}{6}\right) \quad (2)$$

$S(b)$ is the signal intensity at a specific b value, S_0 is the signal intensity at $b = 0\text{ s/mm}^2$, ADC is the apparent diffusion coefficient, D is the diffusion coefficient, and K is the apparent kurtosis coefficient.

Two radiologists, one with 10 years of clinical experience and the other with 4 years of clinical experience in gynecological radiology, blinded to the clinical and pathological diagnosis, analyzed the diffusion data. The ROI was manually drawn on each slice of DW images with a b value of 1400 s/mm^2 to encompass as much tumor area as possible. The role of cysts, hemorrhage, necrosis, and nearby blood vessels were excluded with T2-weighted and contrast-enhanced T1-weighted imaging as guides (Fig. 1). For tumor volume analysis, the area of ROI drawn on each slice of the

Main points

- Volume-based histogram analysis of DKI and conventional DWI parameters could be used as predictors for deep myometrial invasion in endometrial carcinoma.
- The ADC value derived from conventional DWI tended to be lower in the deep myometrial invasion subgroup than in the superficial myometrial invasion subgroup.
- Patients with deep myometrial invasion had significantly lower D values and higher K values than those with superficial myometrial invasion.
- The conventional DWI model had an effectiveness equivalent to that of the DKI model in discriminating deep myometrial invasion.

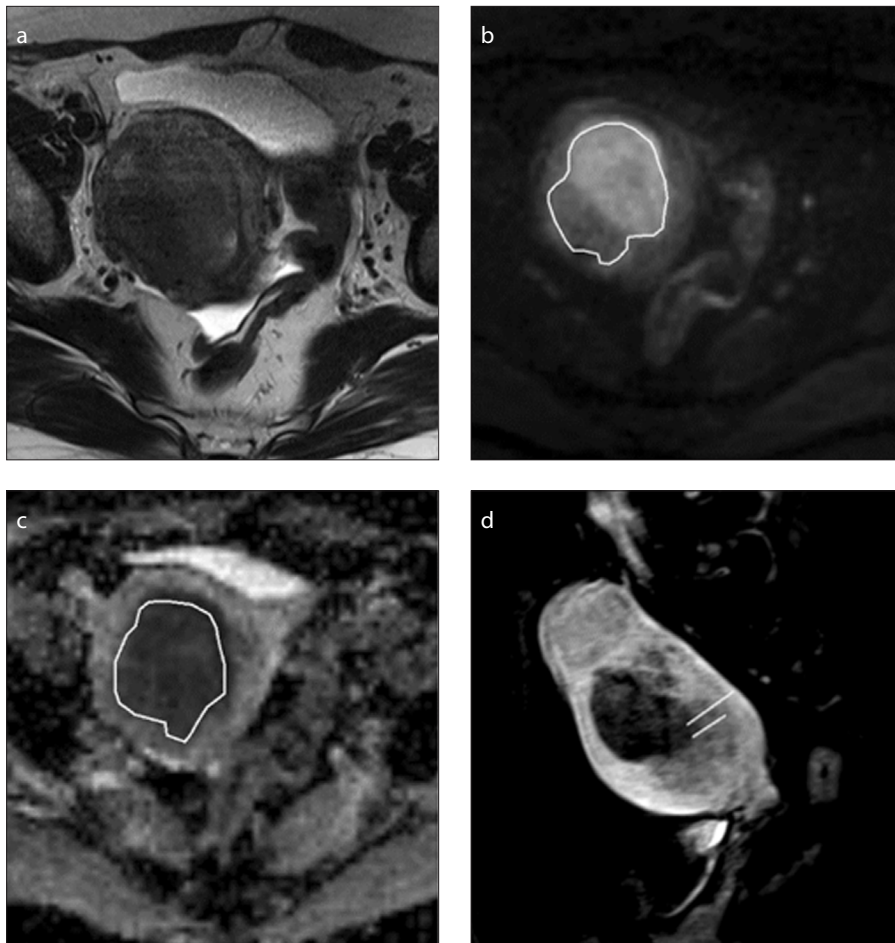


Figure 1. a–d. Delineation of ROI in a 47-year-old woman with endometrioid carcinoma with deep myometrial invasion. It shows low signal intensity on T2-weighted images (a), high signal intensity on corresponding DW images ($b = 1400 \text{ s/mm}^2$) (b) and decreased ADC value of endometrioid carcinoma on ADC map in the uterine cavity (c). Sagittal contrast-enhanced T1-weighted image (d) shows deep myometrial invasion of $>1/2$ depth of myometrium. ROI was drawn to cover the entire tumor based on diffusion-weighted images (b). The T2-weighted imaging (a) and contrast-enhanced T1-weighted imaging (d) were used as references to exclude necrosis, cystic portion, hemorrhage, and surrounding blood vessels.

tumor foci was multiplied by the thickness of each DW image generated the tumor volume of interest (VOI) of each slice, then all of the VOIs were summed to obtain a whole tumor volume which was calculated by the software automatically.

Histogram analysis was conducted based on a two-dimensional plot with x-axes of a bin-size of $1 \times 10^{-6} \text{ mm}^2/\text{s}$ for D and a bin-size of $1 \times 10^{-3} \text{ mm}^2/\text{s}$ for K. The y-axis represents the percentage of tumor volume, which was determined by dividing the frequency in each bin by the total amount of voxels analyzed. Then, cumulative K and D were acquired from their respective histograms using the cumulative number of observations in every one of the bins up to the stated bins. The histogram parameters were obtained from the D and K maps using SPSS

20.0 software (PASW Statistics; SPSS Inc.), and included mean, median, kurtosis (which is a quantification of the “peakedness” of the histogram), skewness (a measurement of the asymmetry of the histogram), and the 10th and 90th percentiles of the tumor K, D, and ADCs (the nth percentile is the point at which n% of the voxel values that form the histogram remained).

Surgical-pathological analysis

Clinical factors were obtained from the patient electronic medical records system, including age and surgical strategies. Pathological information was obtained from the pathological reports. The depth of the myometrial invasion was grouped into two sections: superficial, which we used when there was no myometrial inva-

sion or when it was of less than one-half of the thickness of myometrium, and deep, in which there was invasion to one-half or more of the thickness of the myometrium. The differentiation grade of the tumors (well-differentiated, moderately differentiated, and poorly differentiated) were also determined.

Statistical analysis

All of the measurements were expressed as the mean \pm standard deviation. A two-tailed $P < 0.05$ was considered to be statistically significant. The Kolmogorov-Smirnov’s test was used to determine whether the quantitative parameters were normally distributed. An independent t test was employed to compare data with normal distribution. In all other instances, the Mann-Whitney U test was utilized. The overall ability to differentiate the deep myometrial invasion was evaluated with receiver-operating characteristic (ROC) curve analysis for the parameters that significantly varied among superficial and deep myometrial invasion. The diagnostic activity was measured using the areas under the ROC curves (AUC) according to the technique described in DeLong et al. (22). The specificity and sensitivity were determined at the threshold that maximized the Youden index (Youden index = sensitivity \pm specificity - 1).

The quantifications of both readers were utilized to determine inter-reader reproducibility. The first reader re-assessed all of the images presented in a different order two months after the first assessment in order to calculate the intra-reader reproducibility. As suggested by Koo et al. (23), the two way mixed effects, consistency, single rater intraclass correlation coefficients (ICC) form was used in both inter-reader and intra-reader reproducibility test. The ICC ranged from 0 to 1.00, with values closer to 1.00 indicating better reproducibility: $r < 0.40$ poor, 0.41–0.60 moderate, 0.61–0.80 good, and ≥ 0.81 excellent. The average of measurement results of the two readers were used in the statistical analysis.

All of the statistical analyses were conducted using software MedCalc version 12.1.1.0 for Windows (MedCalc software).

Results

Of the total 118 pathologically confirmed EC patients, 112 were endometrioid adeno-

carcinoma, three were serous papillary adenocarcinoma, one was mucinous adenocarcinoma, one was endometrioid carcinoma with squamous differentiation, and one was clear cell carcinoma. The mean volume of EC was $10.14 \pm 17.11 \text{ cm}^3$ (1.14–120.58 cm^3). The patients' carcinomas were categorized on the American Joint Committee on Cancer (AJCC) scale of well differentiated (n=28, 23.8%), moderately differentiated (n=60, 50.8%), and poorly differentiated (n=30, 25.4%). There were 39 of the 118 patients who had deep myometrial invasion, while 79 patients had superficial myometrial invasion. The detailed information on the clinical and pathological qualities of the study participants are summarized in Table 1.

The average patient age showed no significant difference between the deep myometrial invasion and the superficial myometrial invasion groups (53.72 ± 9.15 vs. 59.72 ± 8.40 , $P = 0.055$). Tumor volume of the deep myometrial invasion group was significantly larger than in the superficial myometrial invasion group ($17.94 \pm 15.76 \text{ cm}^3$ vs. $6.29 \pm 5.40 \text{ cm}^3$, $P = 0.009$). A cutoff value of 12.97 cm^3 was set for tumor volume to differentiate deep myometrial invasion, with an AUC, sensitivity, and specificity of 0.68, 38.5%, and 92.4%, respectively.

Good or excellent intra- and inter-reader agreements were achieved throughout the quantitative measurements of K, D, and ADC parameters. In-depth intra- and in-

ter-reader ICCs for the various DKI and DWI values are shown in Table 2.

In the DKI model, patients with deep myometrial invasion had significantly lower values in the D_{mean} , $D_{10\text{th}}$, and $D_{90\text{th}}$ ($P < 0.001$, $P < 0.001$, and $P = 0.023$), as well as higher values in the K_{mean} and $K_{90\text{th}}$ ($P = 0.002$ and $P = 0.026$) compared with those with superficial invasion. The deep myometrial invasion group had significantly increased D_{skewness} and D_{kurtosis} compared with the superficial myometrial invasion group ($P < 0.001$ and $P = 0.007$, respectively) (Table 3).

In the DWI model, patients with deep myometrial invasion had significantly lower values in ADC_{mean} , $\text{ADC}_{10\text{th}}$, and $\text{ADC}_{90\text{th}}$ compared with those with superficial myometrial invasion ($P = 0.001$, $P = 0.001$, and $P = 0.042$). Simultaneously, the deep myometrial invasion group had significantly increased skewness and kurtosis of ADC values compared with the superficial myometrial group ($P = 0.001$ and $P = 0.03$).

Two representative cases involving superficial and deep myometrial invasion of EC for the comparative analysis of histogram parameters of DKI and conventional DWI are presented in Fig. 2.

Table 4 shows the AUC values for DKI and conventional DWI parameters that were used for discriminating deep myometrial invasion in EC.

Among the histogram parameters of D, $D_{10\text{th}}$ had the highest AUC (AUC=0.72) for differentiating deep myometrial invasion. A cutoff value of $881 \times 10^{-6} \text{ s/mm}^2$ for the $D_{10\text{th}}$ differentiated deep myometrial invasion from superficial invasion with 62.0% specificity and 82.1% sensitivity.

Among the histogram parameters of K, K_{mean} had highest AUC of 0.66 for discriminating deep myometrial invasion from superficial myometrial invasion, with a cutoff value of 940.7×10^{-3} and sensitivity and specificity of 74.4% and 55.7%, respectively.

Among the histogram ADC values, $\text{ADC}_{10\text{th}}$ had the highest AUC (AUC=0.71) for differentiating deep myometrial invasion. A cutoff value of $692 \times 10^{-6} \text{ s/mm}^2$ for $\text{ADC}_{10\text{th}}$ discriminated deep myometrial invasion from superficial invasion with 74.4% sensitivity and 63.3% specificity.

$D_{10\text{th}}$ had a greater AUC value than $\text{ADC}_{10\text{th}}$ in discriminating deep myometrial invasion in EC, although the difference was not statistically significant (0.72 vs. 0.71, $P = 0.35$) (Fig. 3).

Table 1. Clinical and surgical-pathological findings

| Variable | Data (n=118) |
|---|---------------------------|
| Age (years), mean±SD (range) | 55.70±9.31 (34–76) |
| Tumor volume (cm^3), mean±SD (range) | 10.14±17.11 (1.14–120.58) |
| Surgery | |
| Total abdominal hysterectomy | 25 (21.2) |
| Total laparoscopic hysterectomy | 93 (78.8) |
| Revised FIGO staging (2009) | |
| IA | 64 (54.2) |
| IB | 28 (23.7) |
| II | 14 (11.8) |
| IIIA | 0 (0) |
| IIIB | 2 (1.7) |
| IIIC1 | 4 (3.5) |
| IIIC2 | 6 (5.1) |
| Myometrial invasion | |
| Superficial | 79 (66.9) |
| Deep | 39 (33.1) |
| Histological type | |
| Endometrioid | 112 |
| Mucinous adenocarcinoma | 1 |
| Serous papillary carcinoma | 3 |
| Endometrioid with squamous differentiation | 1 |
| Clear cell carcinoma | 1 |
| Histological grade | |
| Well differentiated | 28 (23.8) |
| Moderately differentiated | 60 (50.8) |
| Poorly differentiated | 30 (25.4) |
| Lymphovascular invasion | 26 (22) |
| Lymph node metastasis | 10 (8.5) |

Unless otherwise noted, data are number of patients, with percentages in parentheses. SD, standard deviation.

Table 2. Inter- and intra-reader ICCs for measurements of histogram parameters of D, K, and ADC

| Parameter | Inter-reader ICC | Intra-reader ICC |
|------------------|------------------|------------------|
| Histogram D | | |
| Mean | 0.79 (0.70–0.84) | 0.71 (0.60–0.86) |
| 10 th | 0.80 (0.69–0.84) | 0.78 (0.69–0.87) |
| 90 th | 0.77 (0.68–0.83) | 0.78 (0.69–0.86) |
| Skewness | 0.74 (0.62–0.89) | 0.65 (0.54–0.79) |
| Kurtosis | 0.74 (0.64–0.89) | 0.78 (0.65–0.84) |
| Histogram K | | |
| Mean | 0.75 (0.64–0.78) | 0.77 (0.61–0.86) |
| 10 th | 0.77 (0.66–0.83) | 0.81 (0.77–0.85) |
| 90 th | 0.81 (0.75–0.89) | 0.79 (0.71–0.85) |
| Skewness | 0.72 (0.69–0.81) | 0.74 (0.68–0.80) |
| Kurtosis | 0.81 (0.79–0.86) | 0.77 (0.67–0.85) |
| Histogram ADC | | |
| Mean | 0.76 (0.68–0.84) | 0.72 (0.65–0.83) |
| 10 th | 0.80 (0.73–0.90) | 0.79 (0.74–0.86) |
| 90 th | 0.79 (0.68–0.87) | 0.77 (0.67–0.89) |
| Skewness | 0.73 (0.67–0.85) | 0.70 (0.69–0.85) |
| Kurtosis | 0.77 (0.70–0.85) | 0.76 (0.70–0.85) |

Data in parentheses are 95% confidence intervals.

ICC, intra-class correlation coefficient; ADC, apparent diffusion coefficient; D, apparent diffusion in non-Gaussian distribution, K, apparent kurtosis coefficient; and D_n, K_n, and ADC_n, the nth percentile value of cumulative histograms.

Discussion

The results of our study showed the potential value of DKI and conventional DWI histogram analysis in identifying deep myometrial invasion of EC. Patients with deep myometrial invasion showed lower histogram D, higher histogram K, and greater skewness or kurtosis compared with those with superficial myometrial invasion. Additionally, we determined that the D_{10th}, the K_{mean}, and the ADC_{10th} had better diagnostic effectiveness for discriminating deep myometrial invasion in EC. The AUC of the D_{10th} was slightly higher than the ADC_{10th}.

Recently, numerous studies have examined the potential relationships between ADC values and the degree of myometrial invasion in EC (13, 14, 24, 25). Inoue et al. (13) noted that the minimum ADC value for EC patients with deep myometrial invasion was significantly reduced compared with the ADC value for EC patients with superficial myometrial invasion. Husby et al. (14) also documented that the mean value of ADC was significantly reduced in EC patients with deep myometrial invasion than in patients with superficial or no myometrial invasion. Cao et al. (25) found that the quartile ADC values were higher in subjects

Table 3. Cumulative histogram D, K and ADC parameters of deep and superficial myometrial invasion of patients with endometrial carcinoma

| Parameter | Superficial myometrial infiltration (n=79) | Deep myometrial infiltration (n=39) | P |
|--|--|-------------------------------------|--------|
| D _{mean} (×10 ⁻⁶ mm ² /s) | 1276.6±256.2 | 1098.7±175.6 | <0.001 |
| D _{10th} (×10 ⁻⁶ mm ² /s) | 9347.2±207.5 | 793.2±142.1 | <0.001 |
| D _{90th} (×10 ⁻⁶ mm ² /s) | 1651.5±349.4 | 1497.2.7±326.4 | 0.023 |
| D _{skewness} | 578.8±639.7 | 1073.7±626.3 | <0.001 |
| D _{kurtosis} ^a | 889.3±2209.1 | 2154.5±2675.9 | 0.007 |
| K _{mean} (×10 ⁻³) | 927.1±159.9 | 1002.5±99.1 | 0.002 |
| K _{10th} (×10 ⁻³) | 571.9±213.0 | 601.9±172.2 | 0.45 |
| K _{90th} (×10 ⁻³) | 1260.8±241.1 | 1361.3±194.9 | 0.026 |
| K _{skewness} | -427.1±552.5 | -612.1±561.6 | 0.092 |
| K _{kurtosis} | 1112.2±1236.4 | 1427.4±2377.6 | 0.44 |
| ADC _{mean} (×10 ⁻⁶ mm ² /s) | 975.4±191.8 | 852.6±150.7 | 0.001 |
| ADC _{10th} (×10 ⁻⁶ mm ² /s) | 758.7±148.2 | 665.6±113.9 | 0.001 |
| ADC _{90th} (×10 ⁻⁶ mm ² /s) | 1343.3±275.6 | 1122.4±282.9 | 0.042 |
| ADC _{skewness} | 835.8±874.5 | 1393.8±795.4 | 0.001 |
| ADC _{kurtosis} | 1817.9±4731.7 | 3738.1±3862.0 | 0.03 |

Unless otherwise noted, data are number of mean ± standard deviations and are analyzed by independent t test.

^aData analyzed by Mann-Whitney U test.

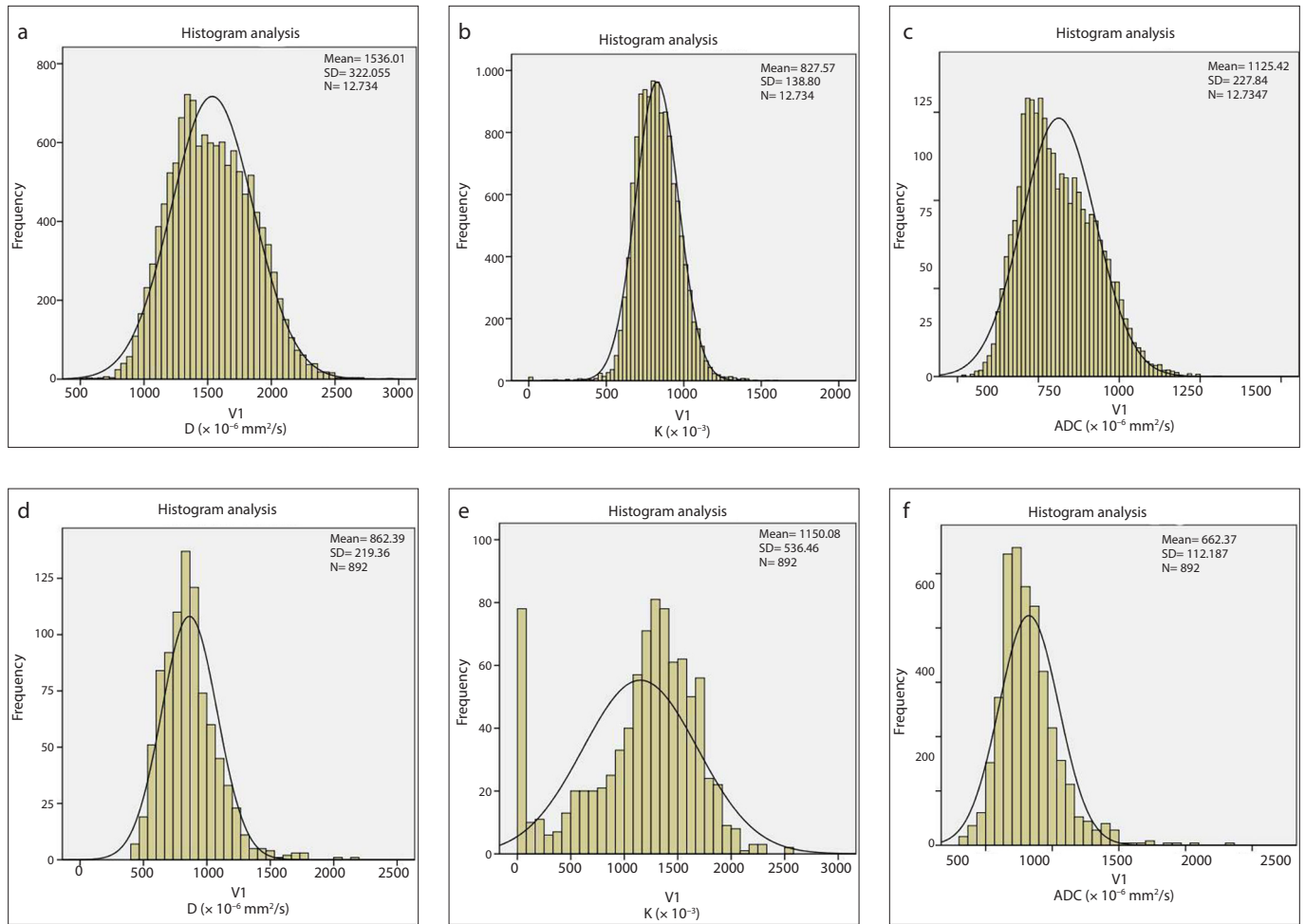


Figure 2. a–f. A comparison of entire tumor volume histogram analysis for D, K, and ADC values between a case with superficial myometrial invasion (a–c) and a case with deep myometrial invasion (d–f) of endometrial carcinoma. The deep myometrial invasion of endometrial carcinoma shows a higher relative frequency at lower D and ADC values, and higher K values when compared with superficial myometrial invasion tumor. The deep myometrial invasion tumor contain more pixels with lower D and ADC values and more pixels with higher K values, which represent higher cellularity, more heterogeneity, and complexity of deep myometrial invasion tumor.

with deep myometrial invasion compared with subjects with superficial myometrial invasion, whereas some researchers did not observe any significant correlation between mean ADC values and the depth of the myometrial invasion (15). Possible explanations for the discrepancy include a limited number of cases involved in the previous research, a lack of optimal range and position of b values in DWI protocols, the use of a single slice of representative ROI instead of entire tumor volume ROIs, and the conventional DWI model not fully reflecting the diffusion characteristics of water molecules. Hence, in the present study, the effectiveness of entire-tumor volume based DKI and conventional DWI for differentiating deep myometrial invasion were examined.

In most of the previous conventional DWI model researches in cervical cancer and EC, the b value was selected as 800 or 1000 s/

mm^2 (12, 13, 25, 26); therefore, we chose a b value of 0 and 800 s/ mm^2 in the conventional DWI model in this study. The quantitative parameters of DKI were shown to be best approximated by utilizing 5 to 7 b values in the range of 300–2000 s/ mm^2 (27). In the female pelvic organs, a maximum b value of 2000 s/ mm^2 would be suitable to obtain adequate signal-to-noise ratio. Thus, we selected the b values of 0, 700, 1400, and 2000 s/ mm^2 based on previous studies (18–21). The present study included 118 patients, which was larger than most of the previous studies.

The present study indicated that patients with deep myometrial invasion had decreased ADC_{mean} , $\text{ADC}_{10\text{th}}$, and $\text{ADC}_{90\text{th}}$ values compared with patients with superficial myometrial invasion. The $\text{ADC}_{10\text{th}}$ had the highest AUC value in predicting deep myometrial invasion compared with the

other parameters of ADC, which is concordant with previous studies (13, 14, 24, 25). It has been reported that the lower percentile of ADC values, such as 10th percentiles, reflected the area of highest cellularity within tumors. The deep myometrial invasion tumors were expected to demonstrate higher cellularity and heterogeneity compared with superficial myometrial invasion tumors, and thus, to have lower ADC values than superficial myometrial invasion tumors.

The DKI model, which is an extension of the conventional DWI model, employs non-Gaussian water diffusion and can more effectively describe *in vivo* tissue microstructural features. D is the corrected form of ADC that is used in non-Gaussian circumstances. Therefore, it was expected that the D values would show a trend similar to ADC. K describes the degree of deviation

Table 4. ROC curve analysis of DKI and DWI histogram parameters for distinguishing deep myometrial invasion of endometrial carcinoma

| Parameters | Cutoff value ^a | AUC | Sensitivity | Specificity |
|--------------------------------|---------------------------|------------------|------------------|------------------|
| D _{mean} | <1226.2 | 0.72 (0.63–0.80) | 82.1 (66.5–92.4) | 58.2 (46.4–69.2) |
| D _{10th} ^b | <881 | 0.72 (0.63–0.80) | 82.1 (66.5–92.4) | 62.0 (50.4–62.7) |
| D _{90th} | <1595.4 | 0.65 (0.55–0.73) | 69.2 (52.4–83.1) | 55.7 (44.1–66.9) |
| D _{skewness} | >771 | 0.72 (0.64–0.81) | 66.7 (49.8–80.9) | 74.7 (63.6–83.8) |
| D _{kurtosis} | >1205 | 0.70 (0.60–0.78) | 56.4 (39.6–72.2) | 79.7 (69.2–88.0) |
| K _{mean} ^b | >940.7 | 0.66 (0.57–0.74) | 74.4 (57.9–86.9) | 55.7 (44.1–66.9) |
| K _{90th} | >1126.7 | 0.64 (0.54–0.72) | 92.3 (79.1–98.5) | 35.4 (25.0–47.0) |
| ADC _{mean} | <890.5 | 0.70 (0.61–0.78) | 69.2 (52.4–83.0) | 65.8 (54.3–76.1) |
| ADC _{10thb} | <692 | 0.71 (0.62–0.79) | 74.4 (57.9–86.9) | 63.3 (51.7–73.9) |
| ADC _{90th} | <1041 | 0.64 (0.55–0.72) | 51.3 (34.8–67.6) | 73.4 (62.3–82.7) |
| ADC _{skewness} | >1097.6 | 0.71 (0.62–0.79) | 71.8 (55.1–85.0) | 72.2 (60.9–81.7) |
| ADC _{kurtosis} | >736.3 | 0.70 (0.64–0.81) | 84.6 (69.5–94.1) | 58.2 (46.6–69.2) |
| ADC _{skewness} | >1097 | 0.65 (0.56–0.74) | 73.1 (52.2–88.4) | 66.3 (55.7–75.8) |

Data are percentage, with range in parentheses.

ROC, receiver operator characteristic; DKI, diffusion kurtosis imaging, DWI, diffusion-weighted imaging; AUC, area under the curve; D, apparent diffusion in non-Gaussian distribution; K, apparent kurtosis coefficient; ADC, apparent diffusion coefficient; D_n, K_n, ADC_n, nth percentile value of cumulative histograms.

^aUnit of 10⁻³ mm²/s for ADC and D, and unit of 10⁻³ for K.

^bThe highest value of histogram D, K and ADC in AUC, Youden index.

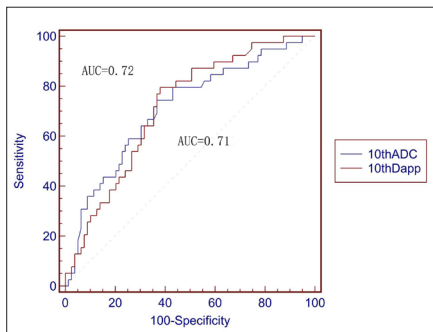


Figure 3. A comparison of the diagnostic ability for discriminating deep myometrial invasion of endometrial carcinoma from superficial myometrial invasion tumors between the 10th percentile of ADC (ADC_{10th}) and the 10th percentile of D (D_{10th}).

from the Gaussian distribution in *in vivo* biological tissue (16, 18). Preliminary studies have demonstrated an inversed correlation between D and K for other neoplasms (16, 20), and the new metric K provides a higher-precision measurement of microstructure complexities of tissues (20, 21). Patients with deep myometrial invasion exhibited decreased D values and increased K values than those with superficial myometrial invasion. This finding indicates an increased heterogeneity and complexity of tumors with deep myometrial invasion (18–21). In addition, we also evaluated the diagnostic accuracy of DKI and standard DWI. Theoretically,

the DKI model describes a more precise characterization of water molecule diffusion in *in vivo* tissues (18–21). However, Roethke et al. (28) demonstrated no significant benefit to DKI in the detection and grading of prostate cancers compared with conventional ADC in the peripheral zone (28). Our study did not demonstrate a significant benefit to DKI-derived parameters compared with the conventional DWI-derived parameters, which is in concordance with Roethke's research. We concluded that the DKI model prohibits an equivalent diagnostic performance in distinguishing the depth of myometrial invasion with the conventional DWI model. This conclusion needs to be further investigated with a large cohort of patients in the prospective studies.

In addition to K, D, and ADC, the distribution of the parameters also provides a pivotal biomarker that reflects the tissue microstructure. We used the entire-tumor volume analysis instead of selected representative ROIs to reflect the true features of the tumors accurately and revealed greater skewness and/or kurtosis of D and ADC values in deep myometrial invasion patients. The increase in skewness or kurtosis indicates higher heterogeneity, as well as complexity of intra-tumorous cellularity. It is well known that increased complexity and heterogeneity of tumors are highly respon-

sible for the local aggressiveness (20, 21). Thus, it is not surprising that patients with deep myometrial invasion exhibited significantly greater skewness and kurtosis of D and ADC values than those with superficial myometrial invasion.

We also demonstrated that the deep myometrial invasion group had significantly greater mean tumor volume than the superficial myometrial invasion group, which is in good concordance with the previous studies (12, 29, 30). Nougaret et al. (12) reported that a tumor volume ratio (TVR) $\geq 25\%$ allows the prediction of deep myometrial invasion with 93% specificity and 100% sensitivity. Ytre-Hauge et al. (29) indicated that the diameter of the anteroposterior tumor could be used independently to predict deep myometrial invasion ($P = 0.001$), and that an anteroposterior diameter > 2 cm indicates deep myometrial invasion with an unadjusted odds ratio of 12.4 ($P < 0.001$). Todo et al. (30) reported that tumor volume represents disease prognosis in EC, and that tumor volume could be utilized as a predictive factor for lymph node metastasis in EC. However, some recent studies regarding the tumor volume or TVR in predicting deep myometrial invasion of EC have drawn somewhat different conclusions. Sahin et al. (31) indicated that tumor size and volume assessed in preoperative MR volumetry cannot predict deep myometrial invasion when used alone. Similarly, Thieme et al. (32) demonstrated that by using a TVR cutoff value of 25%, deep myometrial invasion was predicted with a sensitivity and specificity of 69.2% and 100%, respectively, which was lower than that of DWI. In our study, by using a cutoff value of 12.97 cm³ for tumor volume to predict deep myometrial invasion, the AUC, sensitivity, and specificity were 0.68, 38.5%, and 92.4%, respectively. The optimal threshold value of tumor volume also showed insufficient sensitivity and AUC value in predicting deep myometrial invasion. Therefore, the value of tumor volume in clinical practice for predicting deep myometrial invasion in EC needs to be further investigated with larger sample size and combined together with other parameters.

This evaluation had several limitations. First, this was a retrospective single-center evaluation. However, we believe that the present study might serve as a foundation for future larger, prospective studies. Second, although we have carefully deter-

mined the tumor boundaries and excluded the cystic and necrotic portions, some data were also analyzed for partial volume effects, which resulted in extreme DKI or DWI parameters. We assume the 10th or 90th percentiles of D and K are less prone to be influenced by the partial volume effect. Third, we only assessed the correlation of the histogram parameters D, K, and ADC in relation to the depth of myometrial invasion, and so there is no combination of conventional T2-weighted imaging or contrast-enhanced T1-weighted imaging with histogram parameters of D, K, and ADC values to predict the depth of myometrial invasion. Fourth, there was a lack of subgroup statistical analysis of DKI and DWI according to histological subtypes. Because the cases of non-endometrioid carcinoma were limited (only 6 cases), larger cohort of patients with non-endometrioid carcinomas are needed for further investigation. Finally, tumor volume-based analyses of DWI and DKI were time-consuming. The automated analysis of parametric MRI information could increase the reproducibility of tumor elucidation in the near future.

In conclusion, volume-based DKI and conventional DWI were useful for noninvasively distinguishing deep myometrial invasion in EC. The conventional DWI model had an equivalent effectiveness when compared with the DKI model.

Acknowledgments

The authors are grateful to Dr. Shaofeng Duan for the excellent assistance of statistical analysis.

Conflict of interest disclosure

The authors declared no conflicts of interest.

References

- Siegel R, Naishadham D, Jemal A. Cancer statistics, 2012. *CA Cancer J Clin* 2012; 62:10–29. [CrossRef]
- Singh N, Hirschowitz L, Zaino R, et al. Pathologic prognostic factors in endometrial carcinoma (other than tumor type and grade). *Int J Gynecol Pathol* 2019; 38: S93–S113. [CrossRef]
- Braun MM, Overbeek-Wager EA, Grumbo RJ. Diagnose and management of endometrial cancer. *Am Fam Physician* 2016; 93:468–474.
- Takeuchi M, Matsuzaki K, Nishitani H. Diffusion-weighted magnetic resonance imaging of endometrial cancer: differentiation from benign endometrial lesions and preoperative assessment of myometrial invasion. *Acta Radiol* 2009; 50:947–953. [CrossRef]
- Alektiar KM, McKee A, Lin O, et al. The significance of the amount of myometrial invasion in patients with Stage IB endometrial carcinoma. *Cancer* 2002; 95: 316–321. [CrossRef]
- Binder PS, Mutch DG. Update on prognostic markers for endometrial cancer. *Womens Health* 2014; 10:277–288. [CrossRef]
- Chan JK, Kapp DS. Role of complete lymphadenectomy in endometrioid uterine cancer. *Lancet Oncol* 2007; 8:831–841. [CrossRef]
- Salvesen HB, Haldorsen IS, Trovik J. Markers for individualised therapy in endometrial carcinoma. *Lancet Oncol* 2012; 13:e353–e361. [CrossRef]
- Koplay M, Dogan NU, Erdogan H, et al. Diagnostic efficacy of diffusion-weighted MRI for pre-operative assessment of myometrial and cervical invasion and pelvic lymph node metastasis in endometrial carcinoma. *J Med Imaging Radiat Oncol* 2014; 58:538–546. [CrossRef]
- Gallego JC, Porta A, Pardo MC, Fernández C. Evaluation of myometrial invasion in endometrial cancer: comparison of diffusion-weighted magnetic resonance and intraoperative frozen sections. *Abdom Imaging* 2014; 39:1021–1026. [CrossRef]
- Beddy P, Moyle P, Kataoka M, et al. Evaluation of depth of myometrial invasion and overall staging in endometrial cancer: comparison of diffusion-weighted and dynamic contrast-enhanced MR imaging. *Radiology* 2012; 262:530–537. [CrossRef]
- Nougaret S, Reinhold C, Alsharif SS, et al. Endometrial cancer: combined MR volumetry and diffusion-weighted imaging for assessment of myometrial and lymphovascular invasion and tumor grade. *Radiology* 2015; 276:797–808. [CrossRef]
- Inoue C, Fujii S, Kaneda S, et al. Correlation of apparent diffusion coefficient value with prognostic parameters of endometrioid carcinoma. *J Magn Reson Imaging* 2015; 41:213–219. [CrossRef]
- Husby JA, Salvesen ØO, Magnussen IJ, et al. Tumour apparent diffusion coefficient is associated with depth of myometrial invasion and is negatively correlated to tumour volume in endometrial carcinomas. *Clin Radiol* 2015; 70:487–494. [CrossRef]
- Rechichi G, Galimberti S, Signorelli M, et al. Endometrial cancer: correlation of apparent diffusion coefficient with tumor grade, depth of myometrial invasion, and presence of lymph node metastasis. *AJR Am J Roentgenol* 2011; 197:256–262. [CrossRef]
- Jensen JH, Helpert JA. MRI quantification of non-Gaussian water diffusion by kurtosis analysis. *NMR Biomed* 2010; 23:698–710. [CrossRef]
- Jensen JH, Helpert JA, Ramani A, Lu H, Kaczynski K. Diffusional kurtosis imaging: the quantification of non-Gaussian water diffusion by means of magnetic resonance imaging. *Magn Reson Med* 2005; 53:1432–1440. [CrossRef]
- Yuan J, Yeung DK, Mok GS, et al. Non-Gaussian analysis of diffusion-weighted MR imaging in head and neck at 3T: a pilot study in patients with nasopharyngeal carcinoma. *PLoS One* 2014; 9: e87024. [CrossRef]
- Nogueira L, Brandão S, Matos E, et al. Application of the diffusion kurtosis model for the study of breast lesions. *Eur Radiol* 2014; 24:1197–1203. [CrossRef]
- Rosenkrantz AB, Sigmund EE, Johnson G, et al. Prostate cancer: feasibility and preliminary experience of a diffusional kurtosis model for detection and assessment of aggressiveness of peripheral zone cancer. *Radiology* 2012; 264:126–135. [CrossRef]
- Wang Q, Li H, Yan X, et al. Histogram analysis of diffusion kurtosis magnetic resonance imaging in differentiation of pathologic Gleason grade of prostate cancer. *Urol Oncol* 2015; 33:e15–24. [CrossRef]
- DeLong ER, DeLong DM, Clarke-Pearson DL. Comparing the areas under two or more correlated receiver operating characteristic curves: a nonparametric approach. *Biometrics* 1988; 44:837–845. [CrossRef]
- Koo TK, Li MY. A guideline of selecting and reporting intraclass correlation coefficients for reliability research. *J Chiropr Med* 2016; 15:155–163. [CrossRef]
- Ippolito D, Cadonici A, Bonaffini PA, et al. Semi-quantitative perfusion combined with diffusion-weighted MR imaging in pre-operative evaluation of endometrial carcinoma: results in a group of 57 patients. *Magn Reson Imaging* 2014; 32:464–472. [CrossRef]
- Cao K, Gao M, Sun YS, et al. Apparent diffusion coefficient of diffusion weighted MRI in endometrial carcinoma-relationship with local invasiveness. *Eur J Radiol* 2012; 81:1926–1930. [CrossRef]
- Nakamura K, Imafuku N, Nishida T, et al. Measurement of the minimum apparent diffusion coefficient (ADCmin) of the primary tumor and CA125 are predictive of disease recurrence for patients with endometrial cancer. *Gynecol Oncol* 2012; 124:335–339. [CrossRef]
- Merisaari H, Jambor I. Optimization of b value distribution for four mathematical models of prostate cancer diffusion-weighted imaging using b values up to 2000 s/mm²: simulation and repeatability study. *Magn Reson Med* 2015; 73:1954–1969. [CrossRef]
- Roethke MC, Kuder TA, Kuru TH, et al. Evaluation of diffusion kurtosis imaging versus standard diffusion imaging for detection and grading of peripheral zone prostate cancer. *Invest Radiol* 2015; 50:483–489. [CrossRef]
- Ytre-Hauge S, Husby JA, Magnussen IJ, et al. Preoperative tumor size at MRI predicts deep myometrial invasion, lymph node metastases, and patient outcome in endometrial carcinomas. *Int J Gynecol Cancer* 2015; 25:459–466. [CrossRef]
- Todo Y, Watari H, Okamoto K, et al. Tumor volume successively reflects the state of disease progression in endometrial cancer. *Gynecol Oncol* 2013; 129:472–477. [CrossRef]
- Sahin H, Sarioglu FC, Bagci M, Karadeniz T, Uluer H, Sancı M. Preoperative magnetic resonance volumetry in predicting myometrial invasion, lymphovascular space invasion, and tumor grade: is it valuable in international federation of gynecology and obstetrics stage I endometrial cancer? *Int J Gynecol Cancer* 2018; 28:666–674. [CrossRef]
- Thieme SF, Collettini F, Sehoulı J, et al. Preoperative evaluation of myometrial invasion in endometrial carcinoma: prospective intra-individual comparison of magnetic resonance volumetry, diffusion-weighted and dynamic contrast-enhanced magnetic resonance imaging. *Anticancer Res* 2018; 38:4813–4817. [CrossRef]